

Probing Local Branching Dynamics with Stern-Gerlach Interferometers and Dual Sensing

Xing M. Wang¹

Abstract

We propose a new experimental program to empirically distinguish the Branched Hilbert Subspace Interpretation (BHSI) from the Copenhagen Interpretation (CI) and Many-Worlds Interpretations (MWI) by examining the dynamics of local quantum branching. Our approach uses Stern-Gerlach interferometers (SGIs) equipped with a novel dual sensing technique, combining non-destructive transparent sensors (TSs) and projective opaque detectors (ODs), to test foundational principles in a closed system. The first stage employs a single SGI with dual sensors to search for anomalous "delayed-choice" events that challenge the instantaneous collapse of CI and the global branching of MWI. The second stage involves a full-loop SGI with two TSs and one OD to investigate recoherence phenomena, which would violate both CI and MWI if observed. Finally, the third stage introduces a second full-loop SGI with a test ion to generate an electromagnetic phase shift, enabling discrimination between retrocausal and unitary recoherence mechanisms. Successfully observing these rare anomalies, while without breaking any conservation laws, would offer strong evidence for the local branching framework of BHSI, showing a fuzzy quantum-classical boundary within dual sensing. The proposed experiments are feasible with current trapped-ion and quantum sensing technologies, offering a promising path forward in the ongoing debate over quantum interpretations.

Keywords: Born Rule; Branched Hilbert Subspace Interpretation; Copenhagen Interpretation; Many-Worlds Interpretation; Recoherence; Retrocausality; Stern-Gerlach Interferometer.

Table of Contents:

1. Introduction	1
2. Single Stern-Gerlach Interferometer and Branching Dynamics	3
3. Single Full-Loop Stern-Gerlach Interferometer and Recoherence	7
4. Two Full-Loop Stern-Gerlach Interferometers, Recoherence, and Retrocausality	10
5. Summary and Discussion	13
Abbreviations	14
References	14

1. Introduction

In our previous article [1], we proposed the Branched Hilbert Subspace Interpretation (BHSI), in which a measurement is viewed as a sequence of unitary operators: branching, engaging, and disengaging. The branches are locally decoherent, evolving unitarily and independently, with

¹ Sherman Visual Lab, Sunnyvale, CA 94085, USA; xmwang@shermanlab.com; ORCID:0000-0001-8673-925X

their amplitudes determined by the initial state of the system. They may be conditionally remerged through recoherence before permanently entangling with the surrounding environment. We demonstrated that such locally controlled decoherent-recoherent processes (CDRP) could be seen in quantum teleportation ([2]). We proposed experiments using modern full-loop Stern-Gerlach interferometers [3,4], where one can visualize CDRP, branch weights (encoding the Born rule), and branch-dependent gravitational or electromagnetic (EM) phase shifts. We compared the features of BHSI with those of the Copenhagen Interpretation (CI, [5, 6]), the Many-Worlds Interpretation (MWI, [7-9]), and some other interpretations.

In the follow-up article [10], we revisited Einstein's famous electron diffraction thought experiment, presented at the 1927 Solvay Conference [11,12], to examine the ontological and dynamical implications of quantum measurement. In the single-layer setup, an electron diffracts through a pinhole and is absorbed by an opaque hemispherical array of 1000 position-sensitive sensors. No electron can escape the closed system. This simple arrangement demonstrates that unitary branching can be entirely local, and the Born rule, represented in the branch weight of BHSI, can be visualized. The two-layer hemispheric detector enhances this test by adding a transparent inner detection layer with 200 transparent sensors (TSs) aligned with the 200 opaque detectors (ODs) on the outer array (*dual sensing*). This setup allows the timing of when branching occurs or is completed. Possible anomalous detections, especially misaligned hits (e.g., TS #35 → OD #46), may suggest “*delayed*” choices. BHSI naturally manages such cases through its timely operational sequence. Anomalies like double detections (either inner or outer) would violate single-choice measurement or energy-matter conservation, challenging all interpretations.

In this article, we present a streamlined experimental design based on full-loop Stern-Gerlach interferometers (SGIs) [3, 4] equipped with dual sensing capabilities. The setup combines non-destructive transparent sensors (TSs) and projective opaque detectors (ODs) for a single charged spin-½ particle, enabling direct investigation of local branching dynamics. Such *dual sensing* is already feasible with current technology [10, 13-15].

The experiment has three stages. The first stage uses a single SGI (or the top half of a full-loop SGI) with two integrated dual sensors to examine basic quantum principles (Fig. 1, p. 3). This setup allows for the empirical reproduction and verification of anomalies seen in Einstein's electron diffraction experiment [10], such as TS-OD mismatches (“*delayed choices*”). It also shows how to test the Born rule and conservation laws with this simple arrangement.

The second stage features a full-loop SGI with a TS in each of the two paths and a single OD at the remerging point (Fig. 2, p. 8). This configuration aims to explore potential recoherence. If observed, this would suggest that the branches can remerge and regain coherence even after a local measurement.

The third and final stage adds a second full-loop SGI with a test ion to produce an electromagnetic (EM) phase shift for the electron in the left full-loop SGI (Fig. 3, p. 12). The objective is to determine whether remerging branches align in a way that supports retrocausality or not, based on the EM phase response.

The most compelling anomalies in our experiment are "*delayed choice*" in all three stages and "*recoherence*" in the second and third stages. The observation of these events would clearly distinguish the Branched Hilbert Subspace Interpretation (BHSI) from the Copenhagen Interpretation (CI) and the Many-Worlds Interpretation (MWI). While these anomalies respect established conservation laws, they challenge conventional notions of causality, suggesting a possible *temporal fuzziness or boundary ambiguity* between quantum and classical regimes driven by local branching dynamics within the *dual sensing*.

From now on, we consider abnormal cases *truly observed* if they fall outside the statistical error range and cannot be attributed to device malfunctions. Additional observed results can be used to confirm core quantum principles, including the conservation of mass–energy, charge, and total probability. Recoherence events—especially when combined with controlled EM phase shifts—could offer decisive evidence for or against *retrocausality*, in line with the logic of Wheeler's *delayed-choice thought experiment* and related work [16–19].

Section 5 concludes with a summary and broader discussion.

2. Single Stern-Gerlach Interferometer and Branching Dynamics

In the first stage, we use a single SGI, or the upper half of a full-loop SGI [3]. We insert two compact dual sensors, each containing a transparent sensor (ST) on top of an opaque detector (OD). Hence, the upper SGI forms a closed system (Fig. 1).

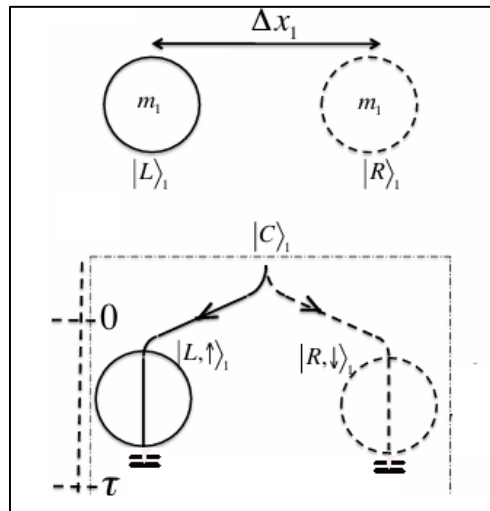


Fig. 1: Single SGI with Two Dual Sensors²

2.1. Technical Feasibility: TS and OD Separation

The dual sensors can be manufactured as integrated compact measurement units. The core of the manufacturing challenge is to build a single, compact unit where the optical path for the TS is precisely aligned with the particle's trajectory just before it strikes the OD. The minimum

² The three figures (including this) presented here are modified versions of the original Fig. 1 in Ref. [4].

distance between the TS's probing region and the OD's active surface could be reduced to sub-millimeter scales with modern microfabrication techniques [13-15]. The limiting factors are the physical size of the components and the need to avoid optical interference.

The TS is a laser-based optical probe, meaning it is a beam of light. Its "footprint" is determined by the size of the laser focus and the collection optics. This can be sub-millimeter. The OD is a physical detector, such as a Microchannel Plate (MCP) or a highly pixelated silicon sensor. These have finite physical thickness. The active surface of an MCP can be placed very close to another object.

The minimum separation distance can be achieved with custom-designed hardware. For example:

- **Integrated Detector Assemblies:** MCPs can be manufactured in compact stacks with very thin front windows. The laser for the TS could be directed through a small hole or from the side, allowing the beam to cross the particle's path and shine on a photodetector.
- **Detector Size:** The physical thickness of a single-stage MCP is typically a few millimeters.
- **Optical Access:** The primary constraint is ensuring the laser beam and the fluorescence photons (if using a fluorescence-based TS) have clear paths without being blocked by the OD's housing. This would require precision engineering of the detector mounts.

Given the typical velocities of cold atoms in SGI experiments, a millimeter separation is sufficient for our purpose. The reaction time of the TS is in the nanosecond-to-microsecond range, and the OD can be even faster, making the time-of-flight between them trivial compared to the overall coherence time of the experiment.

The time window T_W (~ 60 ns) for counting any two successive clicks is set as follows:

$$\tau_{OD} (\sim 1\text{ ns}) < \tau_{TS} (\sim 10\text{ ns}) < T_W (\sim 60\text{ ns}) << 1/f (\sim 1\text{ ms}) \quad (1)$$

Such an arrangement introduces measurement timing uncertainty and blurs the boundary between the quantum and classical worlds. Due to the setup and the measurement timing uncertainty of the dual sensors, along with mostly normal expected outputs, we likely observe some rare, unexpected, and anomalous results.

The Initial State: The ion, located at $|C\rangle_1$, is initialized in the following spin qubit state.

$$|\psi_0\rangle_1 = \cos\theta|\uparrow\rangle_1 + e^{i\phi}\sin\theta|\downarrow\rangle_1 \quad (2)$$

This is achievable via rotated magnetic fields or RF pulses [3]. The next step is decoherence: dropping the ion into the vertical SGI, whose gradient magnetic field entangles spin with momentum, forming a superposition of two paths (left and right, see Fig. 1):

$$|\psi_0\rangle_1 |C\rangle_1 \rightarrow |\psi(0)\rangle_1 = \cos\theta|\uparrow, L\rangle_1 + e^{i\phi}\sin\theta|\downarrow, R\rangle_1 \quad (3)$$

Denote the four readings of the two dual sensors as: $[ST_L, ST_R; OD_L, OD_R]$ (entries are 1 = click, 0 = no click). The outputs of ST and OD can be $[1,0]$, $[0,1]$, $[0,0]$, or $[1,1]$. However, for the TS, it is limited by the mathematical conservation law of total probability (which must sum to 1). In contrast, for the OD, there are physical conservation laws (such as mass, energy, charge, and more), in addition to the total probability.

2.2. Normal (Expected) Outcomes

$$[1,0;1,0] (|\uparrow\rangle_{ST,L} \rightarrow |\uparrow\rangle_{OD,L}) \text{ or } [0,1;0,1] (|\downarrow\rangle_{ST,R} \rightarrow |\downarrow\rangle_{OD,R}) \quad (4)$$

This is the typical, expected result from a quantum measurement. A hit on a transparent sensor (TS) in one path is immediately followed by a hit on the opaque detector (OD) in the same path. The TS-OD pair on the other path does not produce a click. All three interpretations agree with these normal outcomes, but each offers a different explanation.

Interpretations: The output $[1,0;1,0]$ confirms that the left TS acts as a standard measurement device, causing the particle's wave function to decohere and select a single, committed path.

- **CI:** The interaction with the left TS causes the system to collapse into the left dual sensor. The collapse is instant and global: the probability of hitting another path changes to zero instantly, even if the two sensors were located light-years away, indicating that collapse is a faster-than-light action.
- **MWI:** No collapse. The interaction with the left TS causes a branching into two worlds.

$$|\psi\rangle_1 |E\rangle_1 \xrightarrow{TS} \cos\theta |\uparrow\rangle_1 |E_\uparrow\rangle_1 + \sin\theta |\downarrow\rangle_1 |E_\downarrow\rangle_1, \quad \langle E_\uparrow | E_\downarrow \rangle_1 \rightarrow 0 \quad (5)$$

In our world, it activates the left dual sensor, while in the other world, it activates the right dual sensor.

- **BHSI:** No collapse. This situation is identical to the Case 5.1: Aligned Detection (TS #35 \rightarrow OD #35) in [10]. The interaction with a TS causes the system to branch into a single, locally decohered Hilbert subspace corresponding to that path. If the TS reads 1, then it is registered by the OD right after the TS. If the TS reads 0, then the decoherent branch is quickly integrated with the environment without the possibility of triggering the OD. For the outcome $[1,0; 1,0]$, we can write:

$$\text{Left: } t_0 : |\uparrow, L\rangle \xrightarrow{ST} |\uparrow, E_\uparrow\rangle \text{ | reads } |\uparrow\rangle_O \xrightarrow{\text{gap}} |\uparrow, E_\uparrow\rangle \xrightarrow{OD} |\uparrow, E_\uparrow\rangle \text{ | reads } |\uparrow\rangle_O \rightarrow |E\rangle \quad (6)$$

$$\text{Right: } t_0 : |\downarrow, R\rangle \xrightarrow{ST} |\downarrow, E_\downarrow\rangle \xrightarrow{\text{gap}} |\downarrow, E_\downarrow\rangle \rightarrow |E\rangle \quad (7)$$

Below the two dual sensors (outside the closed system), there is no probability of finding the ion anymore due to the conservation laws (mass, energy, charge, etc.).

Born Rule: The frequency with which these outcomes occur, $[1,0;1,0]$ vs. $[0,1;0,1]$, should, over many trials, match the probabilities determined by the initial quantum state. This would serve as another direct verification of the Born rule encoded by the branch weights in BHSI [10].

$$P(\uparrow, L) = P([1,0;1,0]) = \cos^2 \theta, \quad P(\downarrow, R) = P([0,1;0,1]) = \sin^2 \theta \quad (8)$$

2.3. Abnormal (Unexpected) Outcomes

There are many possible abnormal outcomes, some of which are forbidden by global conservation laws (mass-energy, charge, total probability, etc.). The full list of all possible anomalous outcomes is provided here. It offers a framework for interpreting experimental data and a comparative analysis of each category and its implications.

2.3.1. TS-OD Mismatching: $[1,0;0,1]$ ($|\uparrow\rangle_L \rightarrow |\downarrow\rangle_R$) or $[0,1;1,0]$ ($|\downarrow\rangle_R \rightarrow |\uparrow\rangle_L$)

A hit on a TS in one path (e.g., TS_L) is followed by a hit on the OD in the *other* path (OD_R).

Interpretation: Although these abnormal outcomes are rare and unusual, they do not violate any conservation laws. They may occur because the TS reaction time is comparable with the particle transition time between TS and OD, plus the OD reaction time. The closer the TS and OD are, the shorter the OD reaction time, and the higher the chance of it happening.

- **CI:** It is difficult for CI to explain: Instant collapse fixes subsequent outcomes. If truly observed, the standard CI assumptions are violated.
- **MWI:** This outcome is also difficult for MWI to account for, as the TS measurement should have irreversibly split the universe. The final OD detection should then be aligned with the TS detection in that specific world. If swapping truly happens, the standard assumptions of MWI are violated.
- **BHSI (“Delayed Choice”):** For example, the outcome $[1,0; 0,1]$ can be written as:

$$\begin{aligned} \text{Left: } & t_0 : |\uparrow, L\rangle \xrightarrow{\text{ST}} |\uparrow, E_{\uparrow}\rangle \mid \text{reads } \uparrow \rangle_O \xrightarrow{\text{gap}} t_2 : \rightarrow |E'\rangle \\ & \quad (t_0 < t_1 < t_2) \quad (9) \\ \text{Right: } & t_0 : |\downarrow, R\rangle \xrightarrow{\text{ST}} |\downarrow, E_{\downarrow}\rangle \xrightarrow{\text{gap}} |\downarrow, E_{\downarrow}\rangle \xrightarrow{\text{OD}} t_1 : |\downarrow, E_{\downarrow}\rangle \mid \text{reads } \downarrow \rangle_O \rightarrow |E'\rangle \end{aligned}$$

The TS-OD mismatching, a “*delayed-choice*” anomaly where transparent sensors and opaque detectors disagree, mirrors the *misalignment* case: (e.g. TS #35 \rightarrow OD #45) in Section 5.2 of [10]. Although anomalous, it does not violate any conservation laws. Both cases suggest that quantum systems can exhibit temporally local branch resolution, suggesting there exists a fuzzy boundary between the quantum and classical worlds within the dual sensing, where subsystem measurements remain uncertain until a future interaction enforces global consistency.

2.3.2. No TS reading: $[0,0; 0,1]$ or $[0,0,1,0]$.

Neither TS has fired. The dual sensors behave simply like ODs.

Interpretation: It violates the global probability conservation law, which makes it impossible to happen in theory. What if it is truly observed?

- **CI and MWI:** TS's measurement is incomplete, so its action can be ignored. Otherwise, there is no explanation.
- **BHSI (“Uncommitted Choice”):** In addition to device incompleteness, this case may suggest that branching could occur upon hitting the opaque detector before the transparent sensors commit to “read”, implying local and timely dynamic branching, similar to the case of **5.3.2: Missing Inner Detection** in [10]. During the non-destructive measurement process, there may exist a time uncertainty window or a fuzzy classical-quantum boundary, where the global probability conservation might be violated temporarily. However, it is still an open question.

2.3.3. Both TSs reading: [1,1; 0,1] or [1,1,1,0].

Both TSs are committed to reading 1, but only one OD fires. Because both TSs have completed their measurements, none of the three interpretations can explain it naturally. Like the case of **5.3.3** in [10], if this anomaly truly happens, it would raise a question about whether the total probability law could be violated temporarily, as in case **2.3.2**.

2.3.4. Anomalous ODs reading: [x, x; 0,0], or [x, x; 1,1].

They are forbidden by the mathematical probability conservation law (total probability must equal 1) and the physical conservation laws (mass-energy, charge, etc.). No interpretation can explain such outcomes. Like the case of **5.3.4** in [10], if they truly happened, they would challenge the foundations of quantum mechanics.

3. Single Full-Loop Stern-Gerlach Interferometer and Recoherence

Based on BHSI, after a measurement, the branches evolve unitarily and independently. Their recoherence is possible if they remerge before being permanently relocated in the local environment, provided there is no violation of conservation laws (energy, mass, charge, etc.). To explore the possibility of the unique feature of BHSI, we extended the above experiment setup by adding the lower half of the full SGI. We insert two TSs between the upper and lower SGI, and use an OD to detect the final state at the bottom center of the lower SGI (Fig. 2).

To increase the chance of “recoherence,” the crucial condition is that the acceleration or deceleration time Δt is shorter or comparable with the reaction time of the TS ($1 \mu\text{s} \sim 1 \text{ ns}$). The data used in the SGI gravity test are [4]: $\Delta x \sim 10 \mu\text{m}$, $\partial B \sim 10^6 \text{ T}$, $m \sim 10^{-14} \text{ kg}$, and $\Delta t \sim 0.1\text{s}$. Keeping Δx and ∂B unchanged, we can estimate Δt as follows:

$$\Delta x \sim (F_{\partial B} / m) \Delta t^2 / 2 \rightarrow \Delta t \sim \sqrt{m} \rightarrow \Delta t_e \sim \Delta t \sqrt{m_e / m} \quad (10)$$

Therefore, we choose electrons as our charged particle to have $\Delta t_e \sim 1 \text{ ns}$. In alignment with existing high-gradient SGI experiments, we keep the magnetic field gradient on the order of $\partial B \sim$

10^6 T/m. For electrons, this leads to a characteristic acceleration time $\Delta t \sim 1$ ns, which is compatible with the response time of state-of-the-art transparent sensors.

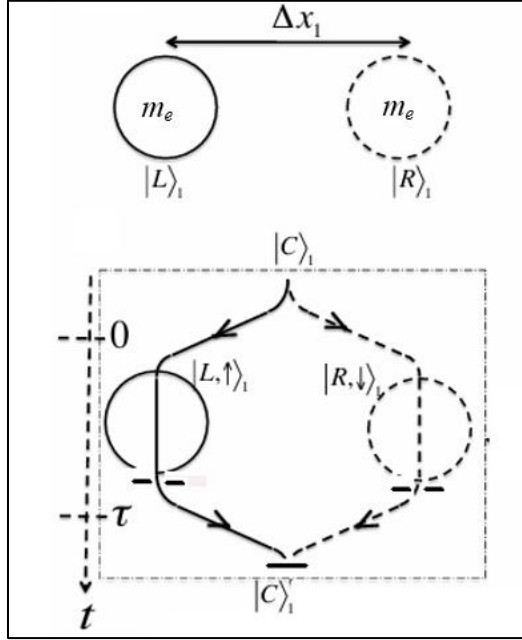


Fig.2: Single Full-Loop SGI with Two TSs and One OD³

The Initial and the controlled decoherent state: The electron, located at $|C\rangle_1$, is initialized in the following spin qubit state.

$$|\psi_0\rangle_1 = \cos\theta|\uparrow\rangle_1 + e^{i\varphi}\sin\theta|\downarrow\rangle_1 = (|\uparrow\rangle_1 + |\downarrow\rangle_1)/\sqrt{2} \quad (\theta = \pi/4, \varphi = 0) \quad (11)$$

The next step is to change it to a locally controlled *decoherent state*: drop the electron vertically into the upper SGI, whose gradient magnetic field entangles spin with momentum, forming a superposition of two paths (left and right) [1, 4]:

$$|\psi(0)\rangle_1 = \cos\theta|\uparrow, L\rangle_1 + e^{i\varphi}\sin\theta|\downarrow, R\rangle_1 = (|\uparrow, L\rangle_1 + |\downarrow, R\rangle_1)/\sqrt{2} \quad (\theta = \pi/4, \varphi = 0) \quad (12)$$

Before inserting the two TSs between the upper and lower SGI, the electron moves down to the lower SGI, and its two branches remerge together by the opposite magnetic gradient. If we measure the electron's state with the OD at the bottom center, we should find that the final state is identical to its initial state, Eq. (11) [1, 4]:

$$|\psi_f\rangle_1 = \cos\theta|\uparrow\rangle_1 + e^{i\varphi}\sin\theta|\downarrow\rangle_1 = (|\uparrow\rangle_1 + |\downarrow\rangle_1)/\sqrt{2} \quad (\theta = \pi/4, \varphi = 0) \quad (13)$$

This is the same Controlled Decoherence-Recoherence Process (CDRP) as described in Section 5.3.1, Eq. (52) of the Ref. [1], with the specialized values of θ and φ .

³ The three figures (including this) presented here are modified versions of the original Fig. 1 in Ref. [4].

Now we insert the two TSs between the upper and lower SGI (Fig. 2). The two TSs and the OD will have different readings. Let us denote the output as: $[TS_L, TS_R; \theta]$. For example, $[1,0; 0]$ means the left TS fires and OD reads $\theta = 0$. The final state can be written as:

$$|\psi_f\rangle_1 = \cos \theta |\uparrow\rangle_1 + e^{i\varphi} \sin \theta |\downarrow\rangle_1 = |\uparrow\rangle_1 \quad (\theta = 0, \varphi = 0) \quad (14)$$

The normal (expected) and anomalous (unexpected) outputs are listed as follows.

3.1. The Normal Outputs:

$[1,0; 0] \rightarrow |\uparrow\rangle$, or $[1,0; \pi/2] \rightarrow |\downarrow\rangle$,

Interpretations: they are expected by all three interpretations, although each offers a different explanation.

CI: The fire of TS_L (TS_R) collapses the wave function to a fixed spin state $|\uparrow\rangle$ ($|\downarrow\rangle$), the other path (with opposite spin state) disappears instantly, then the OD confirms the fixed spin state by reading $\theta = 0$ ($\pi/2$).

MWI: The fire of TS_L splits the current world into two global branches (worlds).

$$|\psi\rangle_1 |E\rangle_1 \xrightarrow{TS} (|\uparrow\rangle_1 |E_\uparrow\rangle_1 + |\downarrow\rangle_1 |E_\downarrow\rangle_1) / \sqrt{2}, \quad \langle E_\uparrow | E_\downarrow \rangle_1 \rightarrow 0 \quad (15)$$

In our world, the left TS reads one (a fixed spin state $|\uparrow\rangle$), the right TS reads zero simultaneously, and the OD confirms the choice by reading $\theta = 0$. At the same time, in the other world (which we cannot communicate with), it is the TS_R that reads one, choosing spin state $|\downarrow\rangle$, while TS_L reads zero, and its OD confirms the choice by reading $\theta = \pi/2$.

BHSI: The fire of TS_L splits the local Hilbert space into two local branches. In the left branch, it has a fixed spin state $|\uparrow\rangle$, and the OD confirms the choice by reading $\theta = 0$. Meanwhile, in the other branch, although its TS_R reads zero (without engaging with the sensor), it does not disappear immediately: it continues to evolve as an independent, decoherent branch for a certain time before finally integrating into its environment without triggering the OD.

$$|\uparrow, L\rangle / \sqrt{2} \xrightarrow{TS_L} |\uparrow_B, E_\uparrow\rangle \text{ | reads } |\uparrow\rangle / \sqrt{2} \xrightarrow{OD} |\uparrow\rangle; \quad |\downarrow, R\rangle / \sqrt{2} \xrightarrow{TS_R} |\downarrow_B, E_\downarrow\rangle / \sqrt{2} \rightarrow |E\rangle \quad (16)$$

3.2. Abnormal (Unexpected) Outcomes

There are potential abnormal outcomes. Some are prohibited by global conservation laws (mass-energy, charge, total probability, etc.). The complete list of all possible anomalous outcomes is provided here. It offers a framework for interpreting experimental data and a comparative analysis of each anomaly and its implications.

3.2.1. Anomalous OD Reading (Remerged Superposition): $[1,0; \pi/4]$ or $[0,1; \pi/4]$.

The left or right TS fires, choosing spin-up or spin-down state, but the OD detects a superposition of both states.

Interpretations: This anomaly does not violate any conservation laws and can clearly distinguish BHSI from CI and MWI.

CI: The fire of TS_L (TS_R) collapses the wave function to a fixed spin state $|\uparrow\rangle$ ($|\downarrow\rangle$), the other path (with opposite spin state) disappears instantly, then there is no chance that OD finds a superposition of the two spin states. It violates CI's fundamental assumption.

MWI: The fire of TS_L splits the current world into two global branches (worlds) as in Eq. (15). Each spin state appears in its own world. There is no chance that the OD finds a superposition of the two spin states. It violates the fundamental assumption of MWI.

BHSI ("Recoherence"): The fire of TS_L splits the local Hilbert space into two local branches. In the left branch, its fixed spin state $|\uparrow\rangle$ is detected by the TS. Meanwhile, the right branch passes the TS without detection and continues evolving as an independent branch. Then the OD finds a superposition of the two spin states by reading $\theta = \pi/4$. It means that the two branches are merged back by the magnetic gradient of the lower SGI – a signal of *recoherence*, which is possible by the fundamental assumptions of BHSI.

$$|\uparrow, L\rangle / \sqrt{2} \xrightarrow{TS_L} |\uparrow, E_\uparrow\rangle \text{ | reads } |\uparrow\rangle / \sqrt{2} \xrightarrow{TS_L} \text{OD}; \quad |\downarrow, R\rangle / \sqrt{2} \xrightarrow{TS_R} |\downarrow, E_\downarrow\rangle / \sqrt{2} \xrightarrow{TS_R} \text{OD} \quad (17)$$

3.2.2. Anomalous TS Reading without Merging: $[0,0; \{0, \pi/2\}]$ or $[1,1; \{0, \pi/2\}]$.

Neither TS fires (or both TSs fire), while the OS reads a single spin state. These anomalies are similar to the cases discussed in Sections 2.3.2 and 2.3.3. The global probability conservation law is violated; no natural explanation from CI, MWI and BHSI. However, in the BHSI, due to local branching dynamics, a time uncertainty or fuzzy zone may exist between the quantum and classical worlds, where probability conservation may be temporarily violated.

3.2.3. Anomalous TS Reading with Merging: $[0,0; \pi/4]$ or $[1,1; \pi/4]$.

Neither TS fires (or both TSs fire), while the OS reads a superposition of two spin states. Similar to cases 2.3.2 and 2.3.3, the global probability conservation law is violated. Suppose both TSs read zero. In that case, the TS's choice might be incomplete or "uncommitted," and the resulting merging can be considered normal for all three interpretations when the TS's action can be ignored, as if it were observed without the TSs, referring to the case described by Eq. (13).

3.2.4. TS-OD Mismatching: $[1,0; \pi/2]$ or $[0,1; 0]$

"Delayed choice". Similar to the case in Section 2.3.1: $[1,0; 0,1]$ or $[0,1; 1,0]$.

4. Two Full-Loop Stern-Gerlach Interferometers, Recoherence, and Retrocausality

Wheeler's delayed-choice thought experiment [16-19] highlights the tension between quantum measurement and temporal causality: If a photon's wave/particle behavior is

determined after it has traversed the interferometer, does the choice "retrocausally" influence its past state? Two interpretations emerge:

- No Retrocausality: The outcome is determined by the experimental configuration at the time of detection (consistent with Copenhagen's "measurement-induced collapse").
- Retrocausality: The future measurement choice affects the past dynamics (e.g., time-symmetric or transactional interpretations).

If recoherence is detected in the single full-SGI experiment, our two-SGIs setup can be extended to detect both recoherence and the EM phase shifts ($\Delta\Phi$). By adding another full-loop SGI on the right with a falling charged particle and keeping the setup of the left full-loop SGI as in the second stage (Fig. 3), we then use the opaque detector (OD) to measure the final state to check if it is a recohered state (a superposition), and whether it has the electromagnetic (EM) phase shift, which was estimated as in Eq. (56) of [1]:

$$\Delta\Phi(\tau) = \frac{q_1 q_2 \tau}{\hbar} \left(\frac{1}{d - \Delta x_1 / 2} - \frac{1}{d + \Delta x_1 / 2} \right) \sim \frac{q_1 q_2 \tau \Delta x_1}{\hbar [d^2 - (\Delta x_1)^2 / 4]} \sim \frac{q_1 q_2 \tau \Delta x_1}{\hbar d^2} \sim 0.2 \text{ rad} \quad (18)$$

Here, we assume $q_1 \sim q_2 \sim -3e$, $d \sim 100 \text{ } \mu\text{m}$, $\Delta x \sim 10 \text{ } \mu\text{m}$, and $\tau \sim 100 \text{ ms}$. In alignment with existing high-gradient SGI experiments [4], we assume a magnetic field gradient on the order of $\partial B \sim 10^6 \text{ T/m}$. For electrons, this leads to a characteristic acceleration time $\Delta t \sim 1 \text{ ns}$, which is compatible with the response time of state-of-the-art transparent sensors. If we use electrons on both SGIs, the resulting electrodynamic (EM) phase shift will be reduced to $\Delta\Phi \sim 0.02 \text{ rad}$, which remains within current interferometric measurement sensitivity.

However, to enhance the electromagnetic phase shift in the dual-SGI setup, we propose replacing the right-arm electron with a heavy spin-0 ion of mass $\sim 10^4$ electron masses and charge $\sim -5e$. This ion is not subject to "split" but falls freely alongside the left-arm electron. Its motion generates a relatively static electric field that interacts with the decoherent branches of the left SGI. As a result, the EM phase shift experienced by the left electron increases to $\Delta\Phi \sim 0.1$ radians, compared to $\Delta\Phi \sim 0.02$ radians when both SGIs employ electrons.

$$\Delta\Phi(\tau) \sim \frac{q_1 q_2 \tau \Delta x_1}{\hbar [d^2 - (\Delta x_1)^2 / 4]} \sim \frac{5e^2 \tau \Delta x_1}{\hbar d^2} \sim 0.1 \text{ rad} \quad (19)$$

This increase significantly improves the detectability of possible recoherence anomalies with EM phase shift. Importantly, no measurements are made on the heavy ion, which acts solely as a moving source of the electric field influencing the left-side quantum system (Fig. 3).

The initial state is set as Eq. (11) for the single SGI setup. It splits into two branches by the magnetic gradient of the left upper SGI, then falls into the space between the upper and lower SGI, experiencing the electric force acting on it by the synchronously falling heavy ion on the right full-loop SGI. Without inserting the two TSs, they merge by the magnetic gradient, forming a superposition with an EM phase shift:

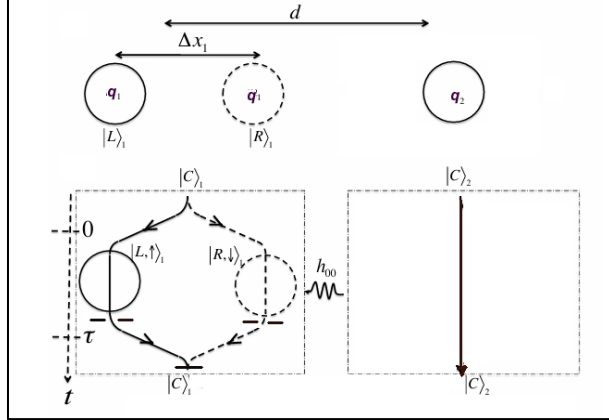


Fig.3: Two Full-Loop SGIs with Two TSs and One OD on the Left SGI⁴

$$|\psi_0\rangle_1 = (|\uparrow\rangle_1 + \beta|\downarrow\rangle_1)/\sqrt{2} \rightarrow U(t)(|\uparrow, L\rangle_1 + |\downarrow, R\rangle_1)/\sqrt{2} \xrightarrow{t=\tau} e^{i\Phi_L(\tau)}[|\uparrow\rangle_1 + e^{i\Delta\Phi(\tau)}|\downarrow\rangle_1]/\sqrt{2} \quad (20)$$

Denoting the outcome by $[\text{TS}_L, \text{TS}_R; \theta, \varphi]$. After inserting the two TSs at the entrance of the lower SGI, we will observe the following outcomes from the two TSs and the OD.

4.1. Normal: $[1,0; 0, 0]$ or $[0,1; \pi/2, 0]$.

Similar to the normal case **3.1**.

4.2. Anomalous:

4.2.1. Anomalous OD Reading with Merging (Recoherence):

Similar to case **3.2.1**.

Without the phase shift: $[1,0; \pi/4, 0]$ or $[0,1; \pi/4, 0]$

With the phase shift: $[1,0; \pi/4, \Delta\Phi]$ or $[0,1; \pi/4, \Delta\Phi]$

4.2.2. Anomalous TS Reading without Merging: $[0,0; \{0, \pi/2\}, 0]$ or $[1,1; \{0, \pi/2\}, 0]$.

Similar to case **3.2.2**.

4.2.3. Anomalous TS Reading with Merging (Recoherence):

Similar to case **3.2.3**.

Without the phase shift: $[0,0; \pi/4, 0]$ or $[1,1; \pi/4, 0]$

With the phase shift: $[0,0; \pi/4, \Delta\Phi]$ or $[1,1; \pi/4, \Delta\Phi]$

4.2.4. TS-OD Mismatching: $[1,0; \pi/2, 0]$ or $[0,1; 0, 0]$.

Similar to the cases in **2.3.1** and **3.2.4**: “Delayed Choice”.

The most interesting case is **4.2.1**, the anomalous OD reading with remerged superposition-recoherence. It does not violate any conservation laws, but can clearly distinguish CI and MWI from BHSI, and also validates the principle of non-retrocausality in quantum mechanics. Suppose no phase shift $\Delta\Phi$ is observed by the OD. In that case, it implies the TS’s measurement erased the independent unitary evolution of the two branches, a signature consistent with retrocausality (where the future measurement choice disrupts past coherence). Conversely, if the OD observes $\Delta\Phi$, it demonstrates that the phase shift is fully determined by local unitary dynamics, independent of the TS’s actions. This would falsify retrocausal interpretations,

⁴ The three figures (including this) presented here are modified versions of the original Fig. 1 in Ref. [4].

affirming that the system's evolution is governed by the pre-measurement history of quantum components [16-19].

5. Summary and Discussion

In this work, we introduce a new experimental program to test the fundamental assumptions of quantum measurement, specifically the processes of local dynamic branching. Our approach uses a multi-stage Stern-Gerlach Interferometer (SGI) setup with dual sensing, combining a non-destructive transparent sensor (TS) and a projective opaque detector (OD), previously utilized in the dual-layer hemispherical detector for the electron diffraction experiment [10]. This design allows direct empirical investigation of how a quantum state evolves under continuous or non-projective measurement.

Our proposed experiment aims to differentiate between the Branched Hilbert Subspace Interpretation (BHSI), the Copenhagen Interpretation (CI), and the Many-Worlds Interpretation (MWI) by testing for various anomalous outcomes. The first stage, involving the upper half of a full-loop SGI with two dual sensors (Fig. 1, p.3), acts as a testbed for foundational principles, focusing on anomalies we call "delayed choices." The observation of such an anomaly in all three stages—where a TS and an OD record conflicting outcomes for the same particle (mismatching, similar to the anomaly of misalignment [10])—would challenge the idea of instantaneous, irreversible collapse in CI and the immediate, global branching posited by MWI.

The second and third stages of our experiment are dedicated to investigating a more profound anomaly: *recoherence*. The second stage uses a single full-loop SGI to test whether a quantum state can be successfully re-established after a local measurement by two TSs (Fig. 2, p. 8). If truly observed, this would provide direct evidence against the conventional view of irreversible decoherence, indicating recoherence may happen before the branches are permanently relocated in the environment. The third stage builds on this by introducing a second SGI with a test ion to generate a measurable electromagnetic phase shift (Fig. 3, p.12). The presence or absence of this phase shift in a recoherent event would serve as a critical test for *non-retrocausality*, which is a core feature of Wheeler's delayed-choice thought experiments.

The two key anomalies, "delayed choices" and "recoherence," challenge conventional views on causality while upholding conservation laws. If truly observed, they would reveal a temporal uncertainty or a fuzzy quantum-classical boundary within dual sensing, directly supporting BHSI's core assumptions. Unlike CI's non-local, instantaneous collapse or MWI's irreversible global branching, BHSI advocates for a local and possibly reversible unitary branching process.

In conclusion, our work (including both the current Stern-Gerlach interferometer designs and the earlier dual-layer hemispheric detector [10]) establishes a practical, technology-based framework for next-generation experiments using dual sensing. By moving beyond traditional "which-path" detection and leveraging modern experimental capabilities, we can directly explore the dynamic aspects of quantum measurement itself. This approach could provide a practical way to test important concepts such as non-retrocausality and conservation laws, while also offering empirical evidence that might shed light on the longstanding debate over quantum

interpretations. These studies could offer a new experimental perspective on the foundations of quantum theory.

Abbreviations

BHSI	Branched Hilbert Subspace Interpretation
CDRP	Controlled Decoherence-Recoherence Process
CI	Copenhagen Interpretation
EM	Electromagnetic
MWI	Many-Worlds Interpretation
OD	Opaque Detector
SGI	Stern-Gerlach Interferometer
TS	Transparent Sensor

References

1. Wang X.M. (2025), Quantum Measurement Without Collapse or Many Worlds: The Branched Hilbert Subspace Interpretation, preprint, DOI: [10.48550/arXiv.2504.14791](https://doi.org/10.48550/arXiv.2504.14791)
2. Ursin R., Jennewein J., Aspelmeyer M., et al., Quantum teleportation across the Danube, Nature 430, 849 (2004), DOI: [10.1038/430849a](https://doi.org/10.1038/430849a). [PDF online](#)
3. Margalit Y, Dobkowski O, Zhou Z., et al. (2021). Realization of a complete Stern-Gerlach interferometer: Towards a test of quantum gravity, Sci. Adv. 2021, V.7-22, DOI: [10.1126/sciadv.abg2879](https://doi.org/10.1126/sciadv.abg2879), on [arXiv](#)
4. Bose S., Mazumdar A., Morley G.W., et al. (2017). A Spin Entanglement Witness for Quantum Gravity, Phys. Rev. Lett. 119, 240401. DOI: [10.1103/PhysRevLett.119.240401](https://doi.org/10.1103/PhysRevLett.119.240401), on [arXiv](#)
5. Bohr, N. (1935). Can a quantum-mechanical description of physical reality be considered complete? Phys. Rev. 48 (8), 696. DOI: [10.1103/PhysRev.48.696](https://doi.org/10.1103/PhysRev.48.696). [PDF online](#)
6. Dirac P. A. M. (1935). The Principles of Quantum Mechanics, 2nd Edition, Oxford University Press. [PDF online](#)
7. Everett, H. (1957). "Relative state" formulation of quantum mechanics. [PDF online](#).
8. Wallace, D. (2012). The Emergent Multiverse. [Oxford Univ. Press: book online](#)
9. Vaidman L. (2022). Why the Many-Worlds Interpretation? Quantum Rep. 2022, 4(3), 264-271, DOI: [10.1103/PhysRevA.71.052105](https://doi.org/10.1103/PhysRevA.71.052105), on [arXiv](#).
10. Wang X. M (2025). Einstein's Electron and Local Branching: Unitarity Does not Require Many-Worlds. DOI: [10.48550/arXiv.2507.16123](https://doi.org/10.48550/arXiv.2507.16123)
11. Bohr N. (1927). General Discussion at the Fifth Solvay Conference: Unpublished Manuscript from Folder Labelled Notes from Solvay Meeting (1927), Niels Bohr Collected Works, [Volume 6, 1985, Pages 99-106](#)
12. Hossenfelder S. (2021). What did Einstein mean by "spooky action at a distance"? A [transcript of the video](#) on [YouTube](#)

13. Gibbons M. J., Hamley C. D, Shih C. -Y, and Chapman M. S. (2011). Nondestructive Fluorescent State Detection of Single Neutral Atom Qubits. *Phys. Rev. Lett.* 106, 133002. DOI: [10.1103/PhysRevLett.106.133002](https://doi.org/10.1103/PhysRevLett.106.133002). [PDF online](#).
14. Hope J. J. and Close J. D. (2005). General limit to non-destructive optical detection of atoms, *Phys. Rev. A* 71, 043822. DOI: [10.1103/PhysRevA.71.043822](https://doi.org/10.1103/PhysRevA.71.043822), on [arXiv](#).
15. Byrnes T., Ebubechukwu O. I. (2021). *Quantum Atom Optics: Theory and Applications to Quantum Technology*. Cambridge University Press, ISBN: 9781108975353. On [arXiv](#).
16. Wheeler J. A., Zurek W. H. (1983). *Quantum Theory and Measurement. I. Questions of Principle*. Princeton University Press. 2016 ISBN: 9780691641027. DOI: [10.1103/PhysRevLett.106.133002](https://doi.org/10.1103/PhysRevLett.106.133002). [PDF online](#).
17. Manning A. G., Khakimov R. I., Dall R. G., et al. (2015), Wheeler's delayed-choice gedanken experiment with a single atom, *Nature Phys* **11**, 539–542, DOI: [10.1038/nphys3343](https://doi.org/10.1038/nphys3343).
18. Ma X., Kofler J., and Zeilinger A. (2016). Delayed-choice gedanken experiments and their realizations. *Rev. Mod. Phys.* 88, 015005. DOI: [10.1103/RevModPhys.88.015005](https://doi.org/10.1103/RevModPhys.88.015005). [arXiv](#).
19. Vedovato F., Agnesi C., Schiavon M., et al. (2017). Extending Wheeler's delayed-choice experiment to Space, *Science Advances* V3, I10. DOI: [10.1126/sciadv.1701180](https://doi.org/10.1126/sciadv.1701180). [arXiv](#).